Alkaline Anion-Exchange Membranes Containing Mobile Ion Shuttles

Xiaolin Ge, Yubin He, Michael D. Guiver, Liang Wu, Jin Ran, Zhengjin Yang, and Tongwen Xu**

Anion-exchange membranes (AEMs) are polymer electrolytes that conduct anions, such as OH^-, Cl^-, SO_4^{2-}, as they contain positively charged groups bound covalently to polymer backbones.[1] Over the last decades, AEMs have been widely used on a large industrial scale in processes such as diffusion dialysis, electrodialysis, electrolysis, for seawater desalination, the treatment of industrial effluents, and chlorine–alkaline production.[2] More recently, to reduce reliance on fossil fuels, there has been increasing interest in the use of AEMs in energy conversion and storage systems, such as reverse electrodialysis,[3] polymer electrolyte fuel cells,[4] microbial fuel cells,[5] and redox flow batteries.[6] In particular, the alkaline anion-exchange membrane fuel cell (AAEMFC) is now considered as one of the most promising green energy-conversion technologies for stationary and mobile applications due to the high fuel conversion efficiency at high pH and low cost stemming from their ability to operate in basic conditions using nonprecious metal catalysts.

However, one key impediment to commercialization is insufficient hydroxide ion (OH^-) conductivity of the central AAEM component. Prior investigations have noted that AAEMs in which the cationic groups are commonly connected to the polymer backbones via short linkages (often $-CH_2-$, referred to as main-chain-type AAEMs) do not exhibit sufficiently high conductivities. Elongating the length of the link should, in principle, enhance the conductivities of AAEMs (referred to as comb-shaped AAEMs) by assisting in the formation of a highly ordered phase-segregated morphology; this morphology generally results from the enthalpy associated with the demixing of incompatible polymer backbones and ionic side chains.[7–20] The ionic side chains tend to self-assemble to construct hydrophilic "channels," wherein OH^- transport is widely considered to proceed via a Grotthuss-type mechanism (schematic illustrated in **Figure 1**A).[21–24] Several researchers have proposed that hydroxide ions are naturally hydrated by hydrogen bonding with water molecules to form different hydration complexes (inactive $OH^-(H_2O)_4$, active $OH^-(H_2O)_3$). The continuous interconversion between hydration complexes driven by fluctuations in the solvation shell of the hydrated ions results in facile OH^- transport (Figure 1A).[25–29] In the "channels" of covalent comb-shaped AAEMs, the cationic groups on the side chains are highly hydrophilic and can freely rotate to enhance such fluctuations via electrostatic interactions with hydrated OH^-; however, the remainder of the side chains are hydrophobic and more rigid, with minor contributions to OH^- conduction.[30–33] Although increasing the ionic content in a covalent comb-shaped AAEM can help to reach the ostensible goal of "higher conductivity," it, in turn, causes undesirable, excessive dimensional swelling from the associated water of hydration. Thus, increasing the mobility of the side chains, rather than the ionic content of AAEMs, is a promising strategy for enhancing the interconversion between hydration complexes without causing excessive dimensional membrane swelling.

The thermal- and pH-triggered mechanical motion of crown ether-based polyrotaxane suggests a fundamentally new direction for developing novel AAEMs with movable side chains.[34,35] Polyrotaxanes represent a significant class of noncovalently bonded polymers, in which linear molecular embedded axles (guests), have mobility through macrocyclic cavities (hosts) in the main chains.[36–40] One of the striking features of these polymers compared with covalently bounded polymers is their structural resemblance to polymer blends, wherein the linear embedded axle components can reversibly vary the aggregation and relative spatial positions with respect to changes in the physical and chemical environment (e.g., temperature and pH). Inspired by this unique molecular architecture, we report for the first time AAEMs containing mobile ion shuttles. Comb-shaped polyrotaxanes were synthesized by threading linear guests containing two dibenzylammonium centers into an aromatic main chain bearing dibenzo[24]crown-8 (DB24C8) cavities via host–guest molecular recognition, followed by confining the guest with bulky ammonium end groups (Figure 1B). The structural characteristics and the beneficial effects of the mobile ion shuttles on OH^- conductivity are investigated in detail.

The comb-shaped polyrotaxane was synthesized as depicted in **Scheme 1**. The poly(crown ether) **1d** was synthesized according to Scheme 1A by polyacylation (see Figure S1 in the Supporting Information).[41–43] The linear side chain guest precursor (**2d**) was synthesized by reacting 1,4-bis(aminomethyl)-benzene with methyl 4-formylbenzoate under reflux in an argon atmosphere for 24 h, followed by reduction with lithium

X. L. Ge, Y. B. He, Dr. L. Wu, J. Ran,
Dr. Z. J. Yang, Prof. T. W. Xu
CAS Key Laboratory of Soft Matter Chemistry
Collaborative Innovation Center of Chemistry
for Energy Materials
School of Chemistry and Materials Science
University of Science and Technology of China
Hefei 230026, P. R. China
E-mail: liangwu8@ustc.edu.cn; twxu@ustc.edu.cn

Prof. M. D. Guiver
State Key Laboratory of Engines
School of Mechanical Engineering
Collaborative Innovation Center of
Chemical Science and Engineering (Tianjin)
Tianjin University
92 Weijin Road, Tianjin 300072, P. R. China

DOI: 10.1002/adma.201506199

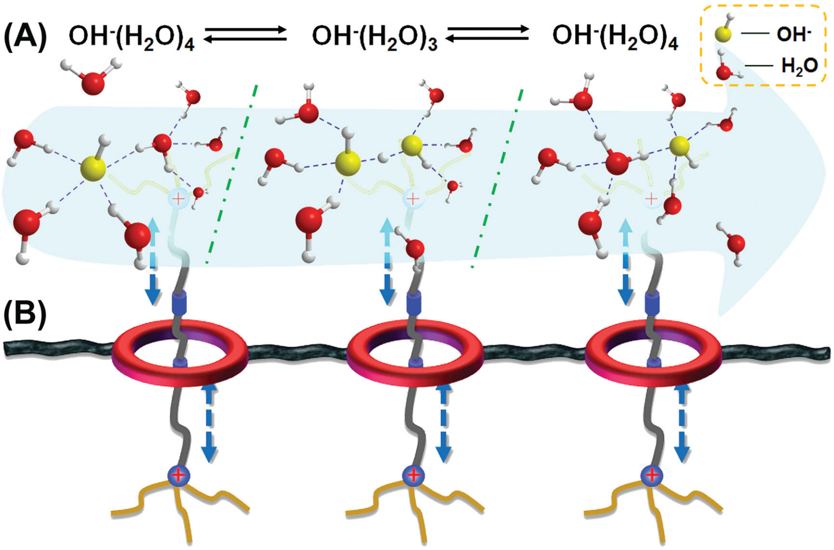

Figure 1. Schematic illustration of (A) hydroxide ion (OH^-) transport via the continuous interconversion between hydration complexes. B) Comb-shaped polymer architecture containing mobile ion shuttles.

aluminum hydride ($LiAlH_4$) (see Scheme S2 and Figure S2 and S3 in the Supporting Information). The terminal hydroxyl and secondary amine groups were then converted into bromomethyl and ammonium groups through sequential reaction with hydrobromic acid (HBr) and ammonium hexafluorophosphate (NH_4PF_6) (see Scheme S2 and Figure S4 in the Supporting Information). The comb-shaped **3d-e•2PF$_6^-$•2Br$^-$** was obtained by first mixing poly(crown ether) **1c** with the ammonium axle component **2e•2PF$_6^-$** and then end-capping the axle termini with bulky tris(2-ethylhexyl)amine (**3a**) to prevent diffusional loss of the side chains (see Scheme S3 and Figure S5 in the Supporting Information). Compared with the ^{1}H NMR spectrum of poly(crown ether) containing no guest molecule in **Figure 2**A, a new ammonium proton signal appears at 9.3 ppm in **3d-e•2PF$_6^-$•2Br$^-$** (Figure 2B), indicating that the dibenzylammonium guest was encircled by the macrocyclic cavities of the poly(crown ether). The percentage of guest incorporation was calculated to be 87.1% by comparing the contents of the ammonium axles and crown ether moieties on the basis of the elemental analysis results. The host–guest polymer is soluble in chloroform (CHCl3), dimethyl sulfoxide, 1-methyl-2-prrolidinone (NMP), and *N,N*-dimethylformamide, but is insoluble in water, even though it contains ammonium moieties.

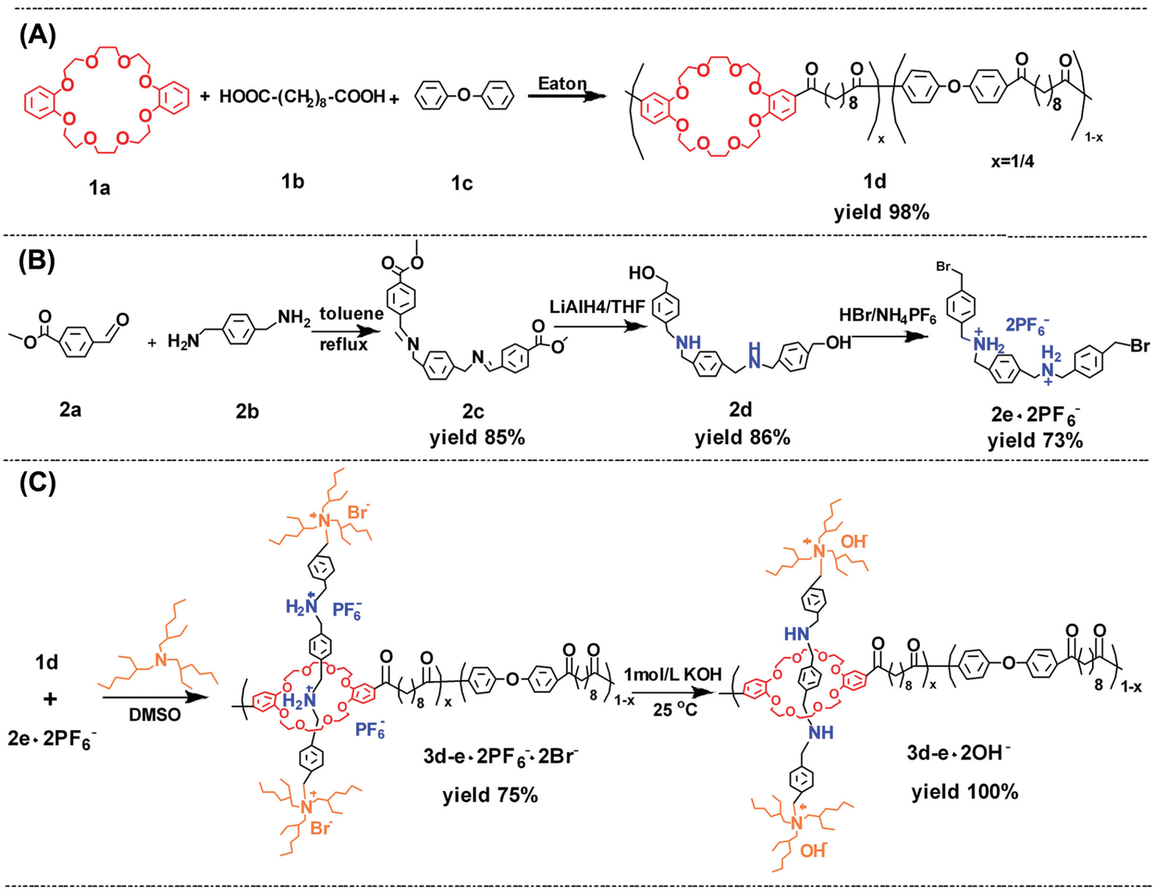

Scheme 1. Synthesis of small molecules and polymers. A) Synthesis of poly(crown ether). B) Synthesis of guest side chain precursor. C) Synthesis of the comb-shaped polyrotaxane AAEM containing mobile ion shuttles.

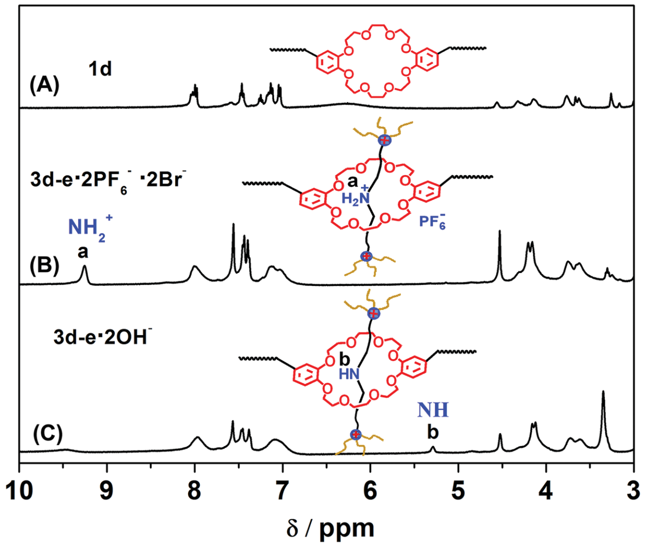

Figure 2. Characterization of polymer structures. A) ^{1}H NMR spectrum of poly(crown ether) **1d**; B) ^{1}H NMR spectrum of polyrotaxane **3d-e•2PF$_6^-$•2Br$^-$** with host–guest interactions. C) ^{1}H NMR spectrum of polyrotaxane **3d-e•2OH$^-$** without host–guest interactions.

The host–guest interaction between the secondary ammonium moieties and crown ether cavities is known to be stimulus-sensitive as a consequence of the relatively low activation energy required for breaking the weak interactions.[34–36] Hence, introduction of a base or heating would be expected to disrupt the host–guest interactions. Upon treatment with 1 M aqueous KOH at 25 °C for 24 h, the dibenzylammonium center was deprotonated back to a neutral amino group, resulting in the disappearance of the dibenzylammonium proton signal at 9.3 ppm and the appearance of a new proton signal at 5.3 ppm arising from the neutral amino groups (Figure 2C; Figure S6, Supporting Information). In addition to the pH stimuli, differential scanning calorimetry (DSC) analysis was also used to investigate the thermal stimuli. The DSC thermogram of **3d-e•2OH$^-$** revealed a broad endothermic peak in the temperature range 40–60 °C (Figure S8, Supporting Information); this peak is attributed to disruption of the host–guest interactions between the crown ether and the dibenzylammonium moieties, suggesting the thermally responsive characteristic of this interaction.

Disrupting this interaction imparts the guest side chains with increased mobility and an increased hydrodynamic radius, which are both expected to accelerate ion transport in the polyrotaxane membrane.

Comb-shaped polyrotaxane-based AAEMs (in the Br$^-$ form) were prepared by solution casting the **3d-e•2PF$_6^-$•2Br$^-$**/NMP solution (8 wt%). To increase the guest chain mobility, the resulting Br$^-$ from AAEM was treated with 1 M aqueous KOH at 25 °C for 24 h to deprotonate the central dibenzylammonium groups back to neutral amino groups, while also converting the termini into the OH$^-$ form for hydroxide ion transport. This membrane is denoted **AAEM$_{3d\text{-}e\bullet 2OH-}$**, and its properties are listed in Table S1 (Supporting Information). The resulting membrane has a relatively low ion-exchange capacity (IEC) of 0.68 mmol g^{-1} as well as water uptake of 18.4%, which endows the membrane an unusually low-dimensional swelling ratio (DSR) of 7.5% at 60 °C.

An interesting transparency-change phenomenon was observed for membranes with different degrees of hydration. As shown in **Figure 3**A, the fully hydrated membranes were translucent after being immersed in water at low temperatures (30 °C, 40 °C) for 24 h; however, they became opaque when hydrated in hot water (50 °C). Interestingly, all of the membranes reverted to transparent after being dried (Figure 3A). The transparency change in the temperatures range of 30 to 80 °C is presented in Figure S7 in the Supporting Information. The multiphase morphology of the hydrated membrane is responsible for this effect. During membrane formation, ionic guest side chains tend to aggregate to form hydrophilic domains, which can adsorb water molecules to form "water pools." Disrupting the host–guest interaction by heating leads to the hydrated membrane structurally resembling a polymer blend, wherein the guest side chain components possibly dissolve in the "water pool" and shuttle independently to a certain extent (Figure 3B). To confirm this assumption, ^{1}H NMR analysis was employed to further evaluate the dynamic behavior of the guest side chains in the hydrated membrane. Figure 3C shows ^{1}H NMR spectra of the membrane/D$_2$O mixture, where the spectra were collected as the temperature increased. The expected proton signals consistent with the guest side chain were observed. The signal intensities continue to increase with temperature from 30 to 50 °C, and then remain constant when further increasing the temperature up to 80 °C (Figure S7, Supporting Information). Moreover, all of the proton signals disappear when the membrane is removed from the D$_2$O (see the bottom spectrum in Figure 3C). This suggests that the mobile guest side chains can dissolve in the hydrated domains but do not undergo diffusive loss from the poly(crown ether) host because of confinement by the bulky end groups. Notably, the hydrophilic domains swell slightly in the hydrated state (DSR of 7.5% at 60 °C in Table S1 in the Supporting Information), which provides sufficient volume for the local side chain shuttling. This exceptional feature is expected to endow the polyrotaxane-based AAEMs with a unique mode of OH$^-$ conductivity without the need for a high concentration of charged anion-exchange groups.

To evaluate the benefits of the mobile shuttles for OH$^-$ conduction, the OH$^-$ conductivities of **AAEM$_{3d\text{-}e\bullet 2OH-}$** were measured as a function of temperature and are depicted in **Figure 4**A. The conductivity increases from 58 mS cm^{-1} at 30 °C and reaches a maximum of 189 mS cm^{-1} at 90 °C. Notably, the conductivity–temperature curve shows a nonlinear increasing trend. The slope of the curve is only 0.71 in the temperature range of 30 to 60 °C, but jumps to 3.27 at the higher temperature range. The profile is distinctly different from that of recently reported covalent comb-shaped AAEMs. As shown in Figure 4B, all curves change in a linear trend, and exhibit lower slopes than that of **AAEM$_{3d\text{-}e\bullet 2OH-}$** at temperatures higher than 60 °C. The thermally triggered mobile shuttle behavior of the guest side chains is responsible for this interesting phenomenon. Base treatment with aqueous KOH disrupts the host–guest interaction between the backbone and the charged center-point of the mobile side chain, by removing the charge on nitrogen. Elevated temperature can provide sufficient energy

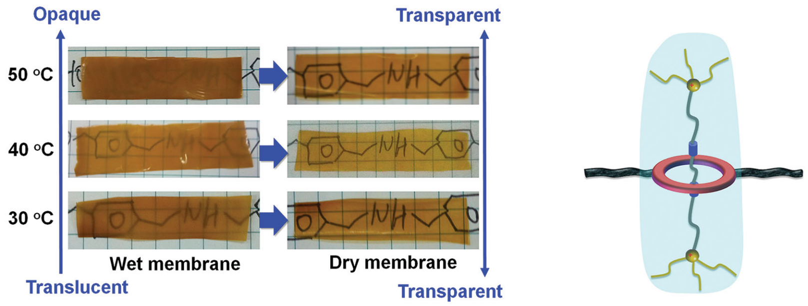

(A) Transparency-change of the membrane in the wet and dry states. (B) "water pool"

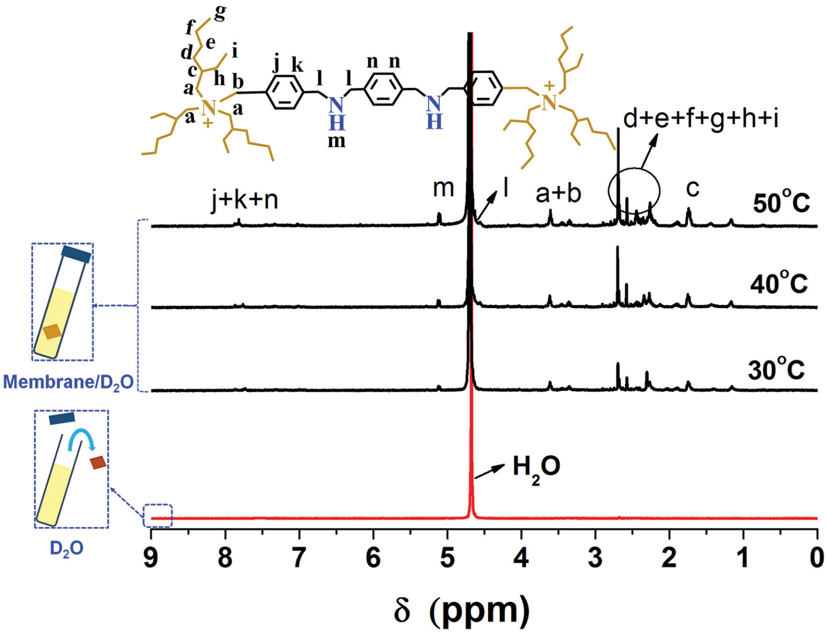

(C) ^1H NMR spectra of membrane/D_2O mixtures

Figure 3. Characterization of charged guest molecules in the hydrated membrane. A) Photographs of hydrated membranes (left) which were immersed in water at different temperatures (30, 40, and 50 °C) for 24 h, respectively, and dry membranes corresponding to the hydrated membranes (right). B) Schematic illustration of the dissolution of hydrophilic side chains in the hydrated membrane. C) ^1H NMR spectra of a membrane/D_2O mixture, where the temperature was increased from 30 to 50 °C, and D_2O after removing membrane at 25 °C (bottom spectrum). The expected proton signals consistent with the guest side chain were observed in the top three dark spectra. Moreover, all of the proton signals disappear when the membrane is removed from the D_2O (the bottom red spectrum). This suggests that the mobile guest side chains can dissolve in the hydrated membrane but do not undergo diffusive loss from the poly(crown ether) host because of confinement by the bulky end groups.

to further promote side chain shuttling. This result is consistent with the DSC thermogram (see Figure S8 in the Supporting Information), in which a phase transition of mobile guest side chains occurs in the temperature range 40–60 °C. Hydroxide ion transport through AAEMs has long been explained by a Grotthuss-type mechanism. The continuous interconversion between hydration complexes (inactive $OH^-(H_2O)_4$, active $OH^-(H_2O)_3$) is driven by fluctuations in the solvation shell of the hydrated ions. We show that the pH-triggered and thermally triggered shuttling of the mobile side chains can significantly increase the solvation-shell fluctuations by breaking the hydrogen bonding in inactive $OH^-(H_2O)_4$ complexes, imparting fast OH^- transport capability. Moreover, Figure 4B also shows that the **AAEM**$_{3d\text{-}e\bullet 2OH-}$ exhibits excellent conductivity—among the highest reported for polymeric membranes to date—but has a correspondingly much lower IEC (0.68 mmol g^{-1}). This result suggests that the dynamic shuttling behavior of the mobile side chains, rather than the ionic content, provides a new approach to achieving high OH^- conduction. It should also be kept in mind that the AAEMs would quickly convert to less conductive CO_3^{2-}/HCO_3^- forms when exposed to CO_2 (or air). Even though OH^- conductivity measured in this study used a set-up probably with a low level of CO_2 exclusion, HCO_3^- conductivity was still measured to evaluate the reliability of the ion shuttle concept obtained from OH^- conductivity data above. As shown in Figure S9 in the Supporting Information, HCO_3^- conductivity at 30 °C is approximately half of OH^- conductivity and increases remarkably with the increase in the temperature. Particularly, it even increases up to 150 mS cm^{-1} at 90 °C, slightly lower than OH^- conductivity at the same temperature (180 mS cm^{-1}). Additionally, the ion shuttle membrane also exhibits favorable conductivity in the Cl^- form, increasing from 30 to 122 mS cm^{-1} with the increase in the temperature in the range of 30 to 90 °C. Hence, the results suggest that this novel ion shuttle AEM is likely to be applicable to a variety of membrane-based technologies involving anion conduction.

Besides high OH^- conductivity, sufficient alkaline stability is also required for the development of AAEMs for AAEMFCs. For quaternary ammonium (QA)-type AAEMs, degradation of the QAs by the OH^- attack is unavoidable (via *β*-hydrogen elimination or direct nucleophilic substitution at *α*-carbon[44,45]). To evaluate the alkaline stability of the **AAEM**$_{3d\text{-}e\bullet 2OH-}$, an accelerated alkaline stability test was performed under harsh conditions (4 M aqueous KOH at 80 °C for 98 h). Chemical structural changes occurring in the membrane during the test were detected by ^1H NMR spectroscopy, as shown in Figure S10 in the Supporting Information. The majority of typical proton signals are maintained after 30 h exposure to the harsh alkali environment. However, in the other spectra corresponding to longer exposure times, the proton signal at 5.3 ppm arising from the neutral amino groups in the mobile side chains disappears, indicating that alkaline degradation occurs. Hofmann elimination of the QA groups caused by OH^- attack is the most likely reason. As discussed in this work, the mobile side chain termini were

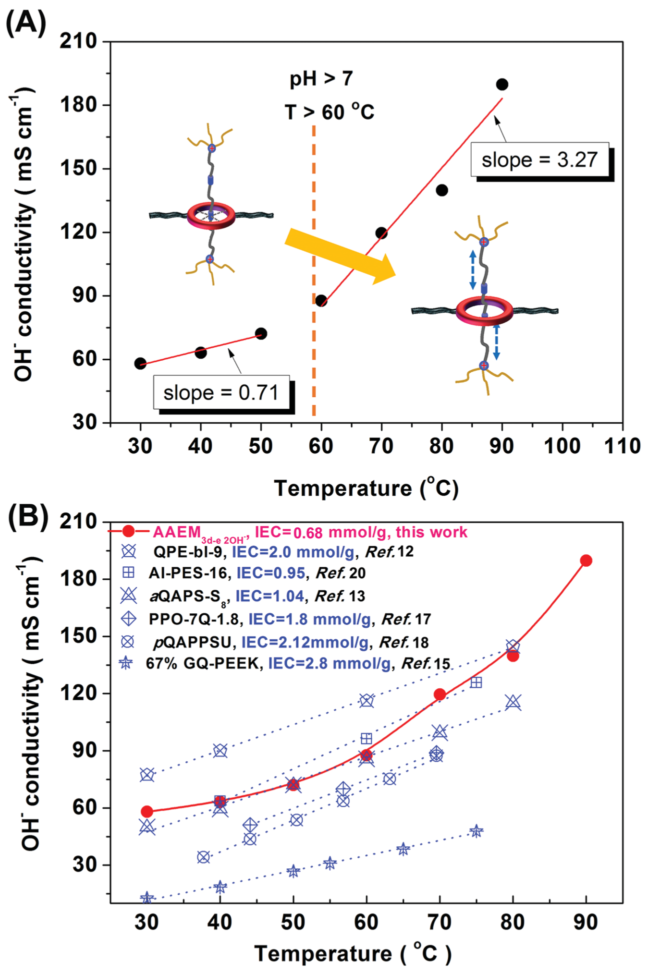

Figure 4. A) Hydroxide ion (OH^-) conductivities of **$AAEM_{3d\text{-}e\bullet 2OH^-}$** as a function of temperature; B) OH^- conductivities of recently reported covalent comb-shaped AAEMs as a function of temperature (**$AAEM_{3d\text{-}e\bullet 2OH^-}$** is shown for comparison).

end-capped by bulky QA moieties. Hence, degradation of the head-groups would result in diffusional loss of the side chains, leading to the disappearance of typical proton signals of the mobile side chains in the corresponding ^1H NMR spectra. Theoretically, the sterically hindered head-groups might impede OH^- attack. However, this effect might be weakened under such a harsh alkaline environment (4 M aqueous KOH at 80 °C). A QA-containing membrane of this type would most likely maintain structural integrity for a longer time if tested under more moderate conditions, e.g., 1 M aqueous KOH at 60 °C (a commonly employed test condition for alkaline stability in the literature). Therefore, one challenge for the ion shuttle design will be to maintain high OH^- conductivity by preventing the diffusion loss of the shuttle in an alkali environment. More efforts will be directed toward improving the alkali stability by introducing more sterically hindered ammonium groups to impede OH^- attack, or replacing the ammonium cations by other more stable alkaline units.

In conclusion, we report a new approach that provides the first example of an AAEM with a mobile ion shuttle, made by threading ionic linear chains into poly(crown ether) main chains via host–guest molecular recognition. The pH- and thermally triggered enhanced mobility of the side chains was observed when the host–guest interaction was disrupted upon treatment with base. While some structural similarities with conventional covalent comb-shaped AAEMs can be made, the polymer architecture of the poly(crown ether)s with pH- and thermally triggered mobile ion shuttles exhibit behavior more resembling polymer blends, wherein the guest side chains can, to a certain extent, shuttle independently in the hydrated state. This exceptional feature endows these AAEMs with excellent conductivity—among the best reported for covalent AAEMs to date—but with a much lower IEC. A systematic study on the relationship between polymer architecture and alkali stability as well as other properties, e.g., dimensional swelling, bicarbonate ion conductivity, single cell performance, are currently in progress.

Supporting Information

Supporting Information is available from the Wiley Online Library or from the author.

Acknowledgements

The authors acknowledge the financial supports from the National Basic Research Program of China (Grant No. 2012CB932802) and the National Natural Science Foundation of China (Grant Nos. 21522607, 21490581, and 21376232).

Received: December 14, 2015
Revised: January 30, 2016

[1] M. A. Hickner, A. M. Herring, E. B. Coughlin, *J. Polym. Sci., Part B: Polym. Phys.* **2013**, *51*, 1727.
[2] H. Strathmann, A. Grabowski, G. Eigenberger, *Ind. Eng. Chem. Res.* **2013**, *52*, 10364.
[3] W. W. Li, H. Q. Yu, *Bioresour. Technol.* **2015**, *196*, 677.
[4] J. R. Varcoe, P. Atanassov, D. R. Dekel, A. M. Herring, M. A. Hickner, P. A. Kohl, A. R. Kucernak, W. E. Mustain, K. Nijmeijer, K. Scott, T. Xu, L. Zhuang, *Energy Environ. Sci.* **2014**, *7*, 3135.
[5] B. E. Logan, M. Elimelech, *Nature* **2012**, *488*, 313.
[6] J. Noack, N. Roznyatovskaya, T. Herr, P. Fischer, *Angew. Chem. Int. Ed.* **2015**, *54*, 9776.
[7] S. Gu, R. Cai, T. Luo, Z. Chen, M. Sun, Y. Liu, G. He, Y. S. Yan, *Angew. Chem. Int. Ed.* **2009**, *48*, 6499.
[8] I. Deavin, S. Murphy, A. L. Ong, S. D. Poynton, R. Zeng, H. Herman, J. R. Varcoe, *Energy Environ. Sci.* **2012**, *5*, 8584.
[9] N. Li, M. D. Guiver, W. H. Binder, *ChemSusChem* **2013**, *6*, 1376.
[10] N. Li, Y. Leng, M. A. Hickner, C. Y. Wang, *J. Am. Chem. Soc.* **2013**, *135*, 10124.
[11] S. S. He, C. W. Frank, *J. Mater. Chem. A* **2014**, *2*, 16489.
[12] N. Yokota, M. Shimada, H. Ono, R. Akiyama, E. Nishino, K. Asazawa, J. Miyake, M. Watanabe, K. Miyatake, *Macromolecules* **2014**, *47*, 8238.
[13] J. Pan, C. Chen, Y. Li, L. Wang, L. Tan, G. Li, X. Tang, L. Xiao, J. Lu, L. Zhuang, *Energy Environ. Sci.* **2014**, *7*, 354.
[14] J. Ran, L. Wu, B. Wei, Y. Y. Chen, T. W. Xu, *Sci. Rep.* **2014**, *4*, 6486.
[15] J. Si, S. Lu, X. Xu, S. Peng, R. Xiu, Y. Xiang, *ChemSusChem* **2014**, *7*, 3389.

[16] A. D. Mohanty, Y. B. Lee, L. Zhu, M. A. Hickner, C. Bae, *Macromolecules* **2014**, *47*, 1973.
[17] H. S. Dang, E. A. Weiber, P. Jannasch, *J. Mater. Chem. A* **2015**, *3*, 5280.
[18] J. Han, Q. Liu, X. Li, J. Pan, L. Wei, Y. Wu, H. Peng, Y. Wang, G. Li, C. Chen, L. Xiao, J. Lu, L. Zhuang, *ACS Appl. Mater. Interfaces* **2015**, *7*, 2809.
[19] W. H. Lee, A. D. Mohanty, C. Bae, *ACS Macro Lett.* **2015**, *4*, 453.
[20] H. N. Rao, S. Nam, T. H. Kim, *J. Mater. Chem. A* **2015**, *3*, 8571.
[21] P. Choi, N. H. Jalani, R. Datta, *J. Electrochem. Soc.* **2005**, *152*, E84.
[22] K. N. Grew, W. K. S. Chiu, *J. Electrochem. Soc.* **2010**, *157*, B327.
[23] M. A. Hickner, *J. Polym. Sci., Part B: Polym. Phys.* **2012**, *50*, 9.
[24] N. Li, M. D. Guiver, *Macromolecules* **2014**, *47*, 2175.
[25] J. S. Wyithe, A. Loeb, *Nature* **2002**, *417*, 923.
[26] R. Ludwig, *Angew. Chem. Int. Ed.* **2003**, *43*, 258.
[27] D. Asthagiri, L. R. Pratt, J. D. Kress, M. A. Gomez, *Proc. Natl. Acad. Sci. USA* **2004**, *101*, 7229.
[28] M. E. Tuckerman, A. Chandra, D. Marx, *Acc. Chem. Res.* **2006**, *39*, 151.
[29] L. Liu, J. Hunger, H. J. Bakker, *J. Phys. Chem. A* **2011**, *115*, 14593.
[30] S. J. Paddison, T. A. Zawodzinski, *Solid State Ionics* **1998**, *333–340*, 113.
[31] J. K. ClarkII, S. J. Paddison, *Electrochim. Acta* **2013**, *101*, 279.
[32] J. A. Elliott, D. S. Wu, S. J. Paddison, R. B. Moore, *Soft Matter* **2011**, *7*, 6820.
[33] A. Vishnyakov, A. V. Neimark, *J. Phys. Chem. B* **2014**, *118*, 11353.
[34] P. R. Ashton, R. Ballardini, V. Balzani, I. Baxter, A. Credi, M. C. T. Fyfe, M. T. Gandolfi, M. Gómez-López, M. V. Martínez-Díaz, A. Piersanti, N. Spencer, J. F. Stoddart, M. Venturi, A. J. P. White, D. J. Williams, *J. Am. Chem. Soc.* **1998**, *120*, 11932.
[35] M. Arunachalam, H. W. Gibson, *Prog. Polym. Sci.* **2014**, *39*, 1043.
[36] J. Wu, K. C. Leung, D. Benitez, J. Y. Han, S. J. Cantrill, L. Fang, J. F. Stoddart, *Angew. Chem. Int. Ed.* **2008**, *47*, 7470.
[37] J. Araki, T. Kataoka, K. Ito, *Soft Matter* **2008**, *4*, 245.
[38] G. De Bo, J. De Winter, P. Gerbaux, C. A. Fustin, *Angew. Chem. Int. Ed.* **2011**, *50*, 9093.
[39] Y. Kohsaka, Y. Koyama, T. Takata, *Angew. Chem. Int. Ed.* **2011**, *50*, 10417.
[40] D. Aoki, S. Uchida, T. Takata, *ACS Macro Lett.* **2014**, *3*, 324.
[41] H. M. Colquhoun, D. F. Lewis, *Polymer* **1988**, *29*, 1902.
[42] M. G. Zolotukhin, M. C. G. Hernandez, A. M. Lopez, L. Fomina, G. Cedillo, A. Nogales, T. Ezquerra, D. Rueda, H. M. Colquhoun, K. M. Fromm, A. Ruiz-Trevino, M. Ree, *Macromolecules* **2006**, *39*, 4696.
[43] Z. H. Zhang, L. Wu, T. W. Xu, *J. Mater. Chem.* **2012**, *22*, 13996.
[44] J. S. Spendelow, A. Wieckowski, *Phys. Chem. Chem. Phys.* **2007**, *9*, 2654.
[45] S. Chempath, B. R. Einsla, L. R. Pratt, C. S. Macomber, J. M. Boncella, J. A. Rau, B. S. Pivovar, *J. Phys. Chem. C* **2008**, *112*, 3179.